
Towards Realistic Hand-Object Interaction with Gravity-Field Based Diffusion Bridge

Miao Xu^{1,2}, Xiangyu Zhu¹, Xusheng Liang², Zidu Wang¹, Jinlin Wu^{1,2}, Zhen Lei^{1,2,3,6*}

¹Institute of Automation, Chinese Academy of Sciences, China

²Centre for Artificial Intelligence and Robotics, Hong Kong Institute of Science, Hong Kong SAR

³School of Artificial Intelligence, University of Chinese Academy of Sciences, China

⁴China Mobile Financial Technology Co., Ltd., China ⁵ZKTeco Co., Ltd., China

⁶School of Computer Science and Engineering, the Faculty of Innovation Engineering, M.U.S.T, Macau, China

{xiangyu.zhu, wangzidu2022, zhangxiaomei2016, zhen.lei}@ia.ac.cn

{miao.xu, jinlin.wu, dong.yi}@cair-cas.org.hk

gaolids@chinamobile.com richard.chen@zkteco.com

Abstract

Existing reconstruction or hand-object pose estimation methods are capable of producing coarse interaction states. However, due to the complex and diverse geometry of both human hands and objects, these approaches often suffer from interpenetration or leave noticeable gaps in regions that are supposed to be in contact. Moreover, the surface of a real human hand undergoes non-negligible deformations during interaction, which are difficult to capture and represent with previous methods. To tackle these challenges, we formulate hand-object interaction as an attraction-driven process and propose a Gravity-Field Based Diffusion Bridge (GravityDB) to simulate interactions between a deformable hand surface and rigid objects. Our approach effectively resolves the aforementioned issues by generating physically plausible interactions that are free of interpenetration, ensure stable grasping, and capture realistic hand deformations. Furthermore, we incorporate semantic information from textual descriptions to guide the construction of the gravitational field, enabling more semantically meaningful interaction regions. Extensive qualitative and quantitative experiments on multiple datasets demonstrate the effectiveness of our method.

1 Introduction

Interaction with objects is an indispensable part of our daily lives, and the most commonly used medium for such interaction is the human hand. Therefore, accurately capturing realistic hand-object interaction states is of critical importance. This capability has broad applications in areas such as gaming, virtual reality (VR), augmented reality (AR), and human-computer interaction [27]. However, due to challenges such as occlusions between the hand and object, existing algorithms often struggle to produce plausible and physically realistic results. Although these methods may suffice for robotic grasping tasks, their physically implausible outputs limit their applicability in high-fidelity scenarios like gaming and virtual reality, where naturalistic is essential.

Recent methods [26, 43, 18, 4, 14] for joint hand-object pose estimation from a single image have shown promising results in modeling hand-object interactions. However, these approaches often focus solely on coarse skeleton-based pose estimation, neglecting the critical relationship between

*Corresponding author.

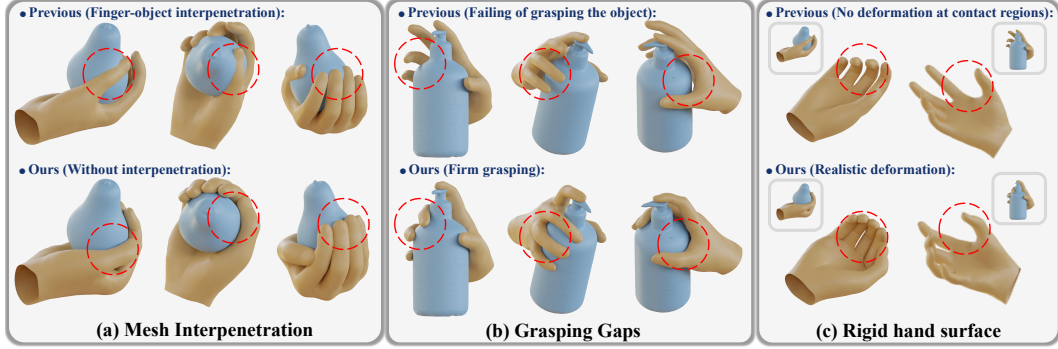


Figure 1: We propose GravityDB to address three key challenges in hand-object interaction: (a) mesh interpenetration between the hand and the object, (b) unsuccessful grasping due to noticeable grasping gaps between the hand and the object, and (c) the inability of previous methods to capture rigid hand surface deformation.

the 3D models of the hand and object. In real-world scenarios, a hand grasping an object undergoes complex surface deformations that are essential for realistic interactions. Ignoring these deformations frequently results in issues such as mesh interpenetration and grasping gaps, even when poses are accurately estimated. As illustrated in Fig. 1(a), even when poses are accurately estimated, the final reconstruction frequently suffers from *mesh interpenetration* artifacts. This occurs when the 3D meshes of the hand and object incorrectly intersect, resulting in visually unrealistic reconstructions. Furthermore, minor pose estimation errors can lead to *grasping gaps*. As shown in Fig. 1(b), the hand fails to grasp the object due to the existence of grasping gaps. Some hand-object reconstruction methods [9, 15, 17] also encounter similar issues due to *rigid hand surface* of the MANO hand model, which lacks the flexibility to represent fine-grained hand deformations, making it difficult to achieve truly realistic interactions. Fig. 1(c) presents these results due to the rigid hand surface.

To address the challenges of unstable hand-object contact in existing interaction modeling methods, such as grasping gaps or mesh interpenetration, we propose a novel Gravity-Field Based Diffusion Bridge (GravityDB). Our approach formulates hand-object contact as a gravitational attraction process, where the surface of object is represented as a zero-potential manifold. A potential energy field is constructed to attract the hand point cloud towards the object surface, effectively correcting unrealistic deformations. To enhance stability and smoothness, we integrate this potential field into a stochastic differential equation (SDE), where the gravitational force ensures convergence toward the object and the diffusion term introduces controlled perturbations that encourage natural shape transitions. Furthermore, to preserve anatomical plausibility, we incorporate a MANO-based structural constraint, guiding the shape of the hand to remain close to the parametric hand model throughout the optimization. This unified framework enables physically plausible, smooth and structure-aware hand deformation, bridging the gap between discrete contact modeling and continuous shape refinement.

To achieve more realistic and effective results, we leverage Large Language Model (LLM) for obtaining contact regions of hand and object to guide the GravityDB. By utilizing text prompts, we extract semantically meaningful contact regions on both the hand and the object, which provide guidance for constructing the gravity field.

To support research on LLM guided hand-object interaction, we build a dataset, which is an extension of existing hand-object interaction datasets [38]. We additionally annotate the contact regions on the 3D point clouds of real hands and objects with instructions, and further refine the original hand meshes to reflect realistic deformation effects. These refined annotations are used as ground truth for evaluation and we will release them to support future research. Please refer to Appendix D for more details.

The contributions of our work can be summarized as follows:

- We propose a novel framework that formulates hand deformation as a diffusion process guided by a Gravity-Field Based Diffusion Bridge. This formulation models the object

surface as a zero-potential manifold and integrates the gravitational force into a stochastic differential equation, enabling smooth, stable, and physically plausible hand deformations.

- We utilize large language model to extract semantically meaningful contact regions on both hands and objects, providing high-level guidance for the Gravity-Field Based Diffusion Bridge and improving contact relevance beyond geometric proximity.
- We validate the effectiveness of our method through extensive experiments on multiple datasets, demonstrating its ability to address the three key challenges, mesh interpenetration, grasping gaps, rigid hand surface and achieving state-of-the-art performance.

2 Related works

Hand-Object Reconstruction. Reconstructing 3D hand-object interactions from images and videos is a well-established research topic [19, 26, 49, 11, 16, 40, 6, 60, 17, 43, 50]. Many existing methods rely on known object templates and focus primarily on estimating the poses of both hands and objects [40, 6, 26, 2, 50]. For instance, Tekin et al. [40] estimate 3D control points for the hand and object in videos, leveraging temporal models to propagate information across frames. Liu et al. [26] propose a semi-supervised pipeline, first generating pseudo-groundtruth annotations from hand-object interaction videos using temporal heuristics, and subsequently using these annotations to train their model. Yang et al. [50] introduce a contact potential field to enhance the quality of hand-object contact modeling. Although these template-based approaches can achieve accurate object pose estimations, their generalization capability to novel objects and in-the-wild videos remains limited due to the reliance on predefined object templates. Alternative methods remove the assumption of known object templates by directly training models using 3D hand-object interaction data [23, 19, 51, 3]. Unfortunately, such methods typically suffer from limited generalization capability, primarily due to the scarcity of available 3D hand-object datasets. Recently, several more generalizable methods [38, 32, 34, 53, 21] have been proposed, leveraging differentiable rendering and data-driven priors. However, these approaches have specific limitations, such as requiring rigid hand-object interactions [21, 32], multi-view observations [34], or category-level supervision for hand-object pairs [53]. In contrast, our proposed method allows for articulated hand motions, relies exclusively on monocular video inputs, and remains agnostic to object categories.

Hand-Object Interaction Denoising. Understanding hand-object interaction (HOI) is critical for interpreting human behaviors, and previous research in this area has primarily addressed data collection [39, 13, 12, 9, 24], reconstruction [42, 48, 34, 54], interaction generation [47, 41, 56, 10, 25], and motion refinement [59, 11, 58, 31]. In contrast, the HOI denoising task specifically aims to remove unnatural artifacts commonly present in interaction sequences. In practical scenarios, denoising models frequently encounter interactions from domains unseen during training, thus requiring robust generalization capabilities. This problem is inherently related to domain generalization, a widely studied topic in machine learning literature [36, 35, 46, 55, 22, 45, 1, 30, 7]. Among various domain-generalization approaches, leveraging domain-invariant representations has emerged as a promising direction, and our work broadly aligns with such methods. However, identifying the exact domain-invariant information relevant to HOI denoising and effectively utilizing this information for generalizable denoising remain challenging open questions. To address these challenges, we focus on designing invariant representations and developing a canonical denoiser that achieves robust cross-domain generalization. Moreover, our research connects to recent studies that exploit data-driven priors to solve inverse problems [37, 28, 44, 29, 5]. Similarly, in the context of HOI denoising, it is crucial to explore fundamental questions regarding the definition of generalizable denoising priors, methods for learning these priors from data, and strategies for effectively leveraging them to refine noisy inputs from diverse distributions. We present our detailed solutions to these issues in the subsequent method section. More recently, GeneOH [27] employed diffusion models for post-processing hand-object interactions. While this approach effectively corrects inaccurate hand trajectories and reduces visual artifacts such as ghosting, it still struggles with mesh interpenetration and unstable grasp configurations due to the inherent challenges of fine-grained modeling.

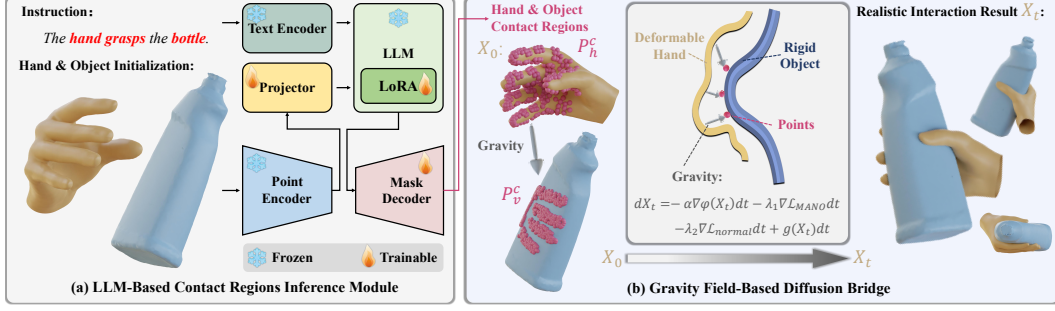


Figure 2: Overview of our method. (a) The LLM-Based Contact Regions Inference Module integrates language instructions and point cloud features to generate probabilistic contact masks. (b) The Gravity-Field Based Diffusion Bridge guides hand deformation via potential field and stochastic diffusion process, regularized by both physical constraints and MANO-based anatomical priors.

3 Methodology

3.1 Overview

Given an input 3D hand point cloud P_h and object point cloud P_v , our goal is to optimize the deformation of the hand to form realistic, physically-plausible contact with the object surface. As illustrated in Fig. 2, we propose a Hierarchical Gravity-Field Based Diffusion Bridge, which models interaction as a smooth stochastic evolution under a multi-scale potential field derived from object geometry and semantic contact intent. To further guide the contact formation process, we introduce a LLM-Based Contact Region Inference Module, which interprets natural language instructions and infers contact probability maps to modulate the gravity field. The framework is staged into coarse-to-fine diffusion steps, incorporating MANO-based hand priors and semantic constraints to ensure anatomical realism and functional plausibility.

3.2 Hierarchical Gravity Field Configuration

We model the object surface contact region P_v^c as a zero-potential manifold, and construct a multi-scale gravitational field to attract relevant hand points. For each hand point $X \in P_h$, the total potential energy is defined as:

$$\varphi(X) = \sum_{l=1}^L \sum_{p \in P_v^c} w_p^{(l)} \cdot k_l \cdot \exp\left(-\frac{\|X - p\|^2}{\sigma_l^2}\right), \quad (1)$$

where $w_p^{(l)} \in [0, 1]$ is derived from the contact mask confidence at scale l , σ_l controls the receptive radius, and k_l is the attraction strength at that scale. The gradient of the potential function $\varphi(X)$ is:

$$\nabla \varphi(X) = - \sum_{l=1}^L \sum_{p \in P_v^c} \frac{2w_p^{(l)} k_l}{\sigma_l^2} (X - p) \cdot \exp\left(-\frac{\|X - p\|^2}{\sigma_l^2}\right). \quad (2)$$

This vector-form gradient represents the resultant force acting on each hand point X within the attraction field. The direction of the force points toward the target point p , while its magnitude is controlled by Gaussian distance decay and multi-scale parameters. It is important to note that, in this work, the object surface is defined as a zero-potential surface. As a result, the attraction force always points toward the surface, regardless of whether a hand point is inside or outside the object. This design ensures that our method is effective in addressing both interpenetration and grasp failure.

3.3 Gravity-Field Based Diffusion Bridge

To enable smooth and stable deformation of the hand point cloud towards plausible contact with the object, we formulate the evolution of each hand point X_t as a stochastic differential equation (SDE),

driven by a combination of physically inspired attraction forces and controlled noise. The base form of the SDE incorporating a diffusion term is given by:

$$dX_t = -\nabla\varphi(X_t)dt + g(X_t)dW_t, \quad (3)$$

where the gravity field term, $-\nabla\varphi(X_t)dt$, models the attractive force induced by a gravitational potential field defined over the object surface. This field directs hand points toward semantically meaningful contact regions while pushing them away from physically implausible or explicitly avoided areas. The potential gradient $\nabla\varphi(X_t)$ acts as a force field derived from a multi-scale Gaussian potential centered around the predicted contact surface. To enhance robustness and exploratory behavior in the deformation process, we introduce structured Brownian motion. The stochastic noise term $g(X_t)dW_t$ represents spatially adaptive noise, helping the system escape poor local minima and promoting smooth convergence. This noise is gradually annealed during the later stages of the process to refine the final hand configuration.

To maintain anatomically plausible hand shapes and prevent deviation from the MANO hand model, we incorporate a shape prior loss:

$$\mathcal{L}_{\text{MANO}} = \|X_t - \mathcal{M}(\theta, \beta)\|^2, \quad (4)$$

where $\mathcal{M}(\theta, \beta)$ denotes the reconstructed hand mesh parameterized by pose θ and shape β . Incorporating this prior, the SDE is refined as:

$$dX_t = -\nabla\varphi(X_t)dt - \lambda_1\nabla\mathcal{L}_{\text{MANO}}dt + g(X_t)dW_t. \quad (5)$$

The additional anatomical regularization term $\lambda_1\nabla\mathcal{L}_{\text{MANO}}dt$ constrains the deformation process to remain within the manifold of physically plausible human hand shapes, effectively preventing joint dislocations and unnatural finger postures.

To avoid isotropic attraction, which may lead to unrealistic contact angles, we introduce a contact normal alignment loss for surface-adjacent hand points:

$$\mathcal{L}_{\text{normal}} = \sum_{X \in P_h^c} \left(1 - \left\langle \mathbf{n}_v, \frac{X - p}{\|X - p\|} \right\rangle \right)^2, \quad (6)$$

where \mathbf{n}_v is the surface normal at the closest point $p \in P_v^c$ on the object. This encourages the approach direction of each hand point to align with the surface normal, leading to more realistic perpendicular contact. Incorporating this into the full SDE yields:

$$dX_t = -\nabla\varphi(X_t)dt - \lambda_1\nabla\mathcal{L}_{\text{MANO}}dt - \lambda_2\nabla\mathcal{L}_{\text{normal}}dt + g(X_t)dW_t. \quad (7)$$

The contact normal alignment term enforces physically realistic contact geometry, ensuring that fingertips or other interacting regions meet the object surface perpendicularly rather than glancing tangentially. This improves both the visual fidelity and the physical plausibility of the final hand-object interaction. We employ scalar hyperparameters λ_1 and λ_2 to control the influence of anatomical and normal-alignment regularizations. These are tuned to balance between physical fidelity and semantic goal adherence, and can be scheduled dynamically across diffusion stages.

To improve convergence, interpretability, and contact stability, we adopt a staged diffusion strategy:

Stage 1: Coarse Guidance. In the initial phase, we apply a low-resolution gravity field with a large receptive radius (σ), which provides a smooth and approximate directionality for the overall hand movement. During this stage, the influence of anatomical priors is relaxed, allowing the hand to approach the semantic contact regions freely. The main goal here is to move the hand into a topologically correct position relative to the object.

Stage 2: Fine Refinement. Once coarse alignment is achieved, we switch to a high-resolution potential field and enforce stricter constraints. The attraction field becomes more localized around inferred contact points, and the MANO prior and normal-alignment loss are strengthened. This stage ensures that individual fingers refine their poses to achieve accurate and stable contact, with enhanced anatomical correctness and collision-free placement.

We numerically solve the SDE using the Euler–Maruyama scheme with an adaptive step size:

$$X_{t+dt} = X_t - \alpha\nabla\varphi(X_t)dt - \lambda_1\nabla\mathcal{L}_{\text{MANO}}dt - \lambda_2\nabla\mathcal{L}_{\text{normal}}dt + g(X_t)\sqrt{dt} \cdot \mathcal{N}(0, I), \quad (8)$$

where α is the gravitational step coefficient and $\mathcal{N}(0, I)$ denotes standard Gaussian noise. The diffusion is terminated when one of the following conditions is satisfied: (i) the gravity field gradient $\|\nabla\varphi(X_t)\|$ falls below a small threshold ϵ , (ii) the iteration count exceeds T_{max} , or (iii) all contact validity criteria are met (no penetrations, all assigned contact regions are occupied).

Table 1: Quantitative comparisons with SOTA diffusion methods on the SHOWMe, GRAB and HO3D. We present Solid Intersection Volume (IV) and Penetration Depth (PD), measuring penetrations, and Proximity Error (PE), evaluating the difference of the hand-object proximity, as well as MPJPE and MPVPE, used to measure hand shape errors. The best and runner-up are highlighted in **bold** and underlined, respectively.

| Dataset | Method | MPJPE (mm, ↓) | MPVPE (mm, ↓) | IV (cm ³ , ↓) | PD (mm, ↓) | PE (mm, ↓) |
|---------|-----------------------|------------------|------------------|-----------------------------|---------------|---------------|
| SHOWMe | Input | 25.42 | 24.93 | 5.13 | 6.02 | 14.77 |
| | TOCH [59] | 15.29 | 15.01 | 2.60 | 2.88 | 3.84 |
| | TOCH w/ Mixstyle [57] | 14.38 | 14.05 | 2.36 | 2.73 | 3.59 |
| | TOCH w/ Aug | 13.22 | 12.87 | 2.15 | 2.22 | 3.47 |
| | GeneOH [27] | <u>10.10</u> | <u>10.21</u> | <u>1.44</u> | <u>1.95</u> | <u>2.81</u> |
| | Ours | 9.74 | 8.23 | 0.62 | 0.77 | 1.53 |
| GRAB | Input | 23.18 | 22.79 | 4.47 | 5.26 | 13.31 |
| | TOCH [59] | 12.39 | 12.15 | 2.10 | 2.16 | 3.13 |
| | TOCH w/ Mixstyle [57] | 13.37 | 13.02 | 2.29 | 2.60 | 3.12 |
| | TOCH w/ Aug | 12.22 | 11.87 | 1.95 | 2.03 | 3.18 |
| | GeneOH [27] | <u>9.08</u> | 9.23 | <u>1.22</u> | <u>1.75</u> | <u>2.54</u> |
| | Ours | 8.91 | <u>10.05</u> | 0.41 | 0.55 | 1.22 |
| HO3D | Input | 27.86 | 27.30 | 5.86 | 6.92 | 16.20 |
| | TOCH [59] | 16.39 | 16.15 | 2.90 | 3.06 | 4.14 |
| | TOCH w/ Mixstyle [57] | 15.35 | 15.02 | 2.67 | 2.91 | 4.01 |
| | TOCH w/ Aug | 14.22 | 13.88 | 2.35 | 2.43 | 3.87 |
| | GeneOH [27] | <u>11.20</u> | 11.31 | <u>1.64</u> | <u>2.15</u> | <u>3.02</u> |
| | Ours | 10.93 | <u>12.07</u> | 0.83 | 0.95 | 1.70 |

3.4 Instruction-Guided Contact Prediction Module

To enable instruction-aware prediction of hand-object contact regions for guiding the GravityDB process, we propose a multimodal contact reasoning module that integrates natural language instructions with spatial features extracted from 3D point clouds. Specifically, the instruction t is encoded into a semantic embedding using a pre-trained large language model (LLM), while the hand point cloud P_h and object point cloud P_v are independently processed by a shared PointNet encoder to extract spatial representations. These two modalities, semantic and spatial, are fused through a multilayer projection network that aligns the language embedding with the geometric features. The resulting joint representation is then fed into a segmentation head to generate soft contact masks over the hand and object point clouds. Formally, the predicted contact regions are given by:

$$P_h^c, P_v^c = \text{LLM}(P_h, P_v, t), \quad (9)$$

The inferred contact regions P_h^c and P_v^c play a central role in modulating the hierarchical gravity field defined over the object surface. By conditioning the gravitational field on these semantically meaningful regions, our method enables contact-aware hand deformation that aligns with both the linguistic intent and physical realism of the interaction. During testing, we let MLLM first see the image, and generate instruction, and this instruction is feed to guide the interaction. It is worth noting that, we do not need additional manuscript instruction by hand.

4 Experiments

4.1 Experiment Setup

Dataset. We primarily conduct qualitative and quantitative experiments on SHOWMe [38], HO3D-V3 [13], and GRAB [39] datasets. The ShOWMe dataset is a hand-object interaction dataset containing 96 videos of 15 diverse users manipulating 42 objects with precise 3D ground truth scans. It provides high-precision submillimeter-accurate 3D shapes for robust training and evaluation in 3D reconstruction, pose estimation, and grasp analysis. The GRAB dataset is a comprehensive full-body motion capture dataset capturing 10 subjects interacting with 51 everyday objects of diverse shapes and sizes. Using MoCap markers, it provides detailed 3D meshes of body pose, facial expressions, hand articulations, and object poses over time. HO3D-V3 consists of RGB videos

Table 2: Quantitative comparisons with SOTA reconstruction methods of interacting hands and objects on the SHOWMe dataset. The best and runner-up are highlighted in **bold** and underlined, respectively. † means that the method uses ground truth contact regions.

| Method | MPJPE (mm, ↓) | MPVPE (mm, ↓) | IV (cm ³ , ↓) | PD (mm, ↓) | PE (mm, ↓) |
|--------------|------------------|------------------|-----------------------------|---------------|---------------|
| HoMan [17] | 25.42 | 24.93 | 5.13 | 6.02 | 14.77 |
| IHOI [52] | 26.13 | 26.10 | 5.40 | 6.30 | 15.20 |
| DiffHOI [54] | 22.35 | 21.00 | 3.50 | 4.80 | 10.50 |
| Hold [8] | 13.21 | 12.00 | 1.85 | 2.10 | 4.00 |
| Ours | <u>9.74</u> | <u>8.23</u> | <u>0.62</u> | <u>0.77</u> | <u>1.53</u> |
| Ours† | 8.69 | 7.90 | 0.58 | 0.72 | 1.42 |

of a hand manipulating a rigid object. The hand is articulated, and it provides 3D annotations for MANO parameters and 6D object poses. HO3D-V3 represents a collection of hand-object interaction videos recorded using RGB-D cameras. The dataset features per-frame annotations for both 3D hand positions and 6D object orientations, derived through an innovative joint optimization methodology.

Evaluation metrics. For hand mesh recovery, our primary metric is the mean per-vertex position error (MPVPE). Additionally, we employ Procrustes Analysis (PA) on the reconstructed mesh and report the PA-PVE after rigid alignment. We also report the mean per joint position error (MPJPE) along with PA-MPJPE. For the interaction between the hand and instrument, we employ several quantifiers, including Solid Intersection Volume (IV) and Penetration Depth to measure penetrations, Proximity Error to assess the discrepancy in hand-object proximity, and Hand-Object (HO) Motion Consistency to evaluate the consistency of the hand-object motion.

4.2 Implementation details

The implementation of our method involves the following steps and configurations. The input to the system consists of an initial 3D hand point cloud and an object point cloud, both aligned in the MANO space. The architecture includes PointNet++ [33] to extract spatial features from the point clouds, the 7B Vicuna as our LLM backbone to process natural language instructions, and a cross-attention mechanism for aligning the semantic features from the text encoder with the spatial features of the point clouds. To efficiently fine-tune the Vicuna backbone for task-specific requirements, we adopt LoRA [20] during training. We utilize $n = 8192$ points and $d = 6$ dimensions for each point cloud, where each point includes features such as spatial coordinates and additional attributes. To optimize the model, we use a combination of Binary Cross-Entropy Loss, which ensures point-level accuracy, and Dice Loss, which enhances the overall quality of predicted masks, that is particularly effective in handling sparse masks and addressing data imbalance in hand-object interaction tasks. The model is optimized using the AdamW optimizer with a learning rate of 10^{-5} over 3 epochs. We also apply data augmentation techniques, including random rotations, translations, and scaling.

The Gravity-Field Based diffusion bridge is implemented using the Euler-Maruyama scheme with adaptive step sizes. During the coarse guidance phase (Stage 1), we set the initial potential field scale to $\sigma_{\text{coarse}} = 0.2$ to create a smooth attraction landscape. In Stage 2, we refine the field by reducing the scale to $\sigma_{\text{fine}} = 0.05$ and increase the weights for the MANO shape prior and surface normal alignment losses. Specifically, the loss weights are set to $\lambda_1 = 0.5$ for the MANO shape prior, and $\lambda_2 = 0.2$ for the surface normal alignment term. The update step size is $\alpha = 0.01$. Each iteration updates the hand point cloud based on the combined forces from the gravity field, shape priors, and noise components. The diffusion process is iterated until one of the stopping conditions is met: the potential gradient falls below $\epsilon = 1 \times 10^{-4}$, the maximum number of diffusion steps $T_{\text{max}} = 150$ is reached, or physical plausibility is verified. The hyperparameters λ_1 , λ_2 , and α were tuned through cross-validation on a subset of the dataset to balance convergence speed and accuracy.

4.3 HOI Denoising Comparison

We evaluated our method against state-of-the-art denoising approaches on the SHOWMe, GRAB, and HO3D datasets, focusing on frames where the hand is already grasping the object to emphasize shape reconstruction and address issues like penetration and failure to grasp. TOCH w/ Mixstyle is a variant of TOCH [59], created by combining it with a general domain generalization method,

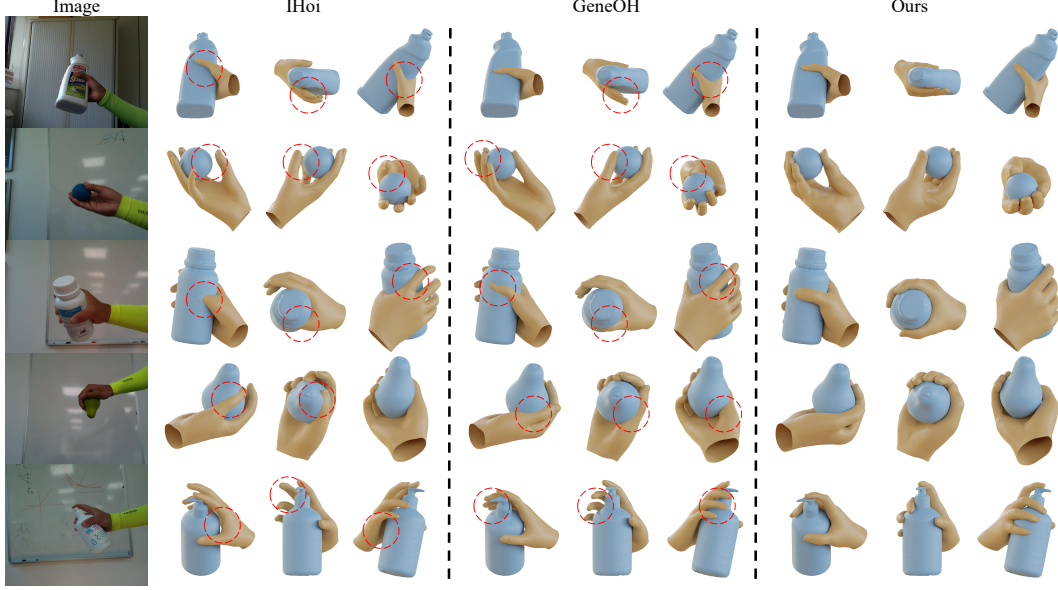


Figure 3: Comparative results with previous methods on SHOWMe. Since the reconstructed object meshes from IHoi are generally of low quality, we use the ground-truth object mesh across all methods to provide a fair and intuitive comparison. Our method demonstrates significantly better performance compared to previous approaches.

MixStyle [57]. TOCH w/ Aug was trained on the GRAB dataset. The input uses hands reconstructed from HoMan and the ground truth objects.

As shown in Table 1, our method consistently outperforms state-of-the-art baselines across key metrics, including MPJPE and MPVPE (measuring hand shape errors), IV and PD (assessing hand-object penetrations), PE (evaluating hand-object proximity), and HOMC (measuring hand-object motion consistency). HOMC, in particular, evaluates the temporal consistency of hand and object motion, which is critical for realistic interaction modeling.

On the SHOWMe dataset, our approach achieves the lowest error in MPJPE (9.74 mm) and MPVPE (8.23 mm), significantly reducing penetration depth (PD: 0.77 mm) and proximity error (PE: 1.53 mm). Similarly, on the GRAB dataset, our method demonstrates superior results, particularly in HOMC (5.29 mm²), highlighting its ability to maintain consistent hand-object motion. On the HO3D dataset, our method excels in handling challenging shapes, achieving the lowest penetration depth (PD: 0.95 mm) and strong overall performance.

These results demonstrate our method’s ability to reconstruct accurate hand deformations in grasping scenarios while effectively resolving issues like penetration and spatial gaps. However, its reliance on ground-truth object shapes for evaluation may limit its applicability in scenarios where object reconstructions are also noisy or incomplete.

4.4 HOI Reconstruction Comparison

Our method demonstrates superior performance compared to state-of-the-art reconstruction approaches on the SHOWMe dataset, as shown in Table 2. Specifically, our method achieves the best results across key metrics such as MPJPE, MPVPE, IV, PD, and PE, significantly reducing errors compared to HoMan and other baselines. The Ours[†] configuration, which uses ground-truth contact regions, highlights the robustness of our method under ideal conditions, serving as an upper bound for performance. These results reflect the effectiveness of our approach in reducing penetrations and improving hand-object alignment.

It is worth noting that the hand mesh ground truth in the SHOWMe dataset has been refined by us to better reflect realistic deformation. This ensures a more accurate evaluation of deformation quality and interaction metrics. Additionally, to ensure fair and consistent comparisons, we use the

Table 3: Ablation studies on the SHOWMe dataset. The best and runner-up are highlighted in **bold** and underlined, respectively.

| Method | MPVPE (mm, ↓) | IV (cm ³ , ↓) | PE (mm, ↓) |
|----------------------------------------|------------------|-----------------------------|---------------|
| Input | 24.93 | 5.13 | 14.77 |
| Ours w/o Gravity | 14.36 | 1.65 | 4.30 |
| Ours w/o $\mathcal{L}_{\text{MANO}}$ | 17.43 | 2.40 | 6.10 |
| Ours w/o $\mathcal{L}_{\text{normal}}$ | <u>12.18</u> | <u>1.05</u> | <u>2.50</u> |
| Ours | 8.23 | 0.62 | 1.53 |

Table 4: Comparisons of using contact regions obtained from different methods on the SHOWMe dataset.

| Method | MPVPE (mm, ↓) | IV (cm ³ , ↓) | PE (mm, ↓) |
|--------------|------------------|-----------------------------|---------------|
| Input | 24.93 | 5.13 | 14.77 |
| Ours w/ Gene | 18.21 | 2.90 | 8.60 |
| Ours w/ Ray | 15.32 | 1.85 | 5.10 |
| Ours w/ PLLM | <u>8.23</u> | <u>0.62</u> | <u>1.53</u> |
| Ours w/ GT | 7.90 | 0.58 | 1.42 |

ground-truth object mesh across all methods, as reconstructed object meshes often exhibit varying quality. While this approach focuses on hand-object interaction metrics, it does not evaluate object reconstruction performance, which is beyond the scope of this work.

In Fig. 3, we present visualization results from different viewpoints. Our method effectively resolves interpenetration issues, as evident from the clear separation between the hand and object surfaces. Additionally, the reconstructed hand poses exhibit anatomically plausible configurations, particularly in grasping scenarios where fingers align naturally with the object surface. This demonstrates the benefits of incorporating the MANO shape prior and proximity alignment losses.

4.5 Ablation Study

Table 3 presents the ablation studies conducted on SHOWMe to evaluate the effectiveness of different components in our method. The initialization uses HoMan for the hand and ground truth objects.

Ours w/o Gravity employs only the contact region guidance, similar to the approach used in TOCH, without leveraging the gravity field to refine hand-object interactions. **Ours w/o $\mathcal{L}_{\text{MANO}}$** omit the anatomical regularization term $\lambda_1 \nabla \mathcal{L}_{\text{MANO}} dt$, removing constraints that ensure the deformation process remains within the manifold of physically plausible human hand shapes. **Ours w/o $\mathcal{L}_{\text{normal}}$** weakens the enforcement of physically realistic contact geometry by excluding the contact normal alignment term.

As shown in Table 3, each module contributes significantly to our method’s overall performance. Removing $\mathcal{L}_{\text{MANO}}$ leads to a substantial increase in MPVPE (from 17.43 mm to 8.23 mm), highlighting its importance in maintaining anatomically plausible hand shapes. Similarly, omitting $\mathcal{L}_{\text{normal}}$ results in notable degradation in IV (from 1.05 cm³ to 0.62 cm³), demonstrating its role in reducing penetrations and ensuring realistic contact geometry. The gravity field further facilitates effective diffusion by guiding hand-object alignment, improving all metrics.

Table 4 presents the results of diffusion guided by different contact region generation methods. **Ours w/ Gene** computes contact regions using nearest-point calculations [27], while **Ours w/ Ray** employs ray-based methods [59]. **Ours w/ PLLM**, our proposed method, utilizes a large language model (LLM) to identify semantically meaningful contact regions, leveraging textual descriptions and object semantics. **Ours w/ PLLM** achieves results closer to ground truth, with a PE of 1.53 mm, compared to 8.60 mm and 5.10 mm for Gene and Ray, respectively. This demonstrates the advantage of incorporating semantic information for accurate contact region identification. Fig. 4 illustrates the contact regions predicted by the large language model.

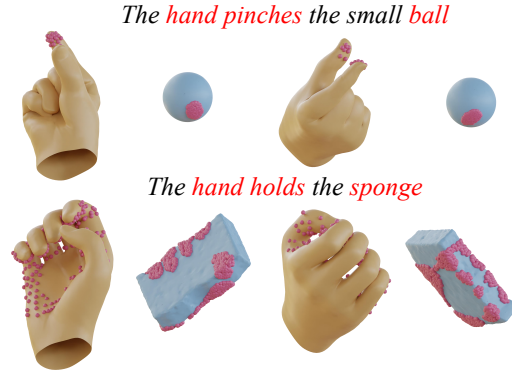


Figure 4: Visualization results of the LLM-Based Contact Regions Inference Module.

5 Conclusion

In this paper, we introduce a novel Gravity-Field Based Diffusion Bridge (GravityDB) for reconstructing physically plausible hand-object interactions by formulating the problem as an attraction-driven process. Our method combines a Gravity-Field Based diffusion bridge with language-guided contact region inference to address common issues in hand-object interaction, such as interpenetration and unrealistic gaps. Through extensive experiments on SHOWMe, GRAB, and HO3D datasets, we demonstrated that our approach significantly outperforms existing methods in terms of hand shape accuracy, physical plausibility, and motion consistency. The effectiveness of each component was validated through comprehensive ablation studies, confirming that our physics-based formulation, coupled with semantic guidance from language instructions, enables more accurate and natural hand-object interactions while maintaining physical constraints.

References

- [1] Gilles Blanchard, Gyemin Lee, and Clayton Scott. Generalizing from several related classification tasks to a new unlabeled sample. *Advances in neural information processing systems*, 24, 2011.
- [2] Zhe Cao, Ilija Radosavovic, Angjoo Kanazawa, and Jitendra Malik. Reconstructing hand-object interactions in the wild. In *ICCV*, pages 12417–12426, 2021.
- [3] Zerui Chen, Shizhe Chen, Cordelia Schmid, and Ivan Laptev. gSDF: Geometry-driven signed distance functions for 3d hand-object reconstruction. In *CVPR*, pages 12890–12900, 2023.
- [4] Zerui Chen, Yana Hasson, Cordelia Schmid, and Ivan Laptev. Alignsdf: Pose-aligned signed distance fields for hand-object reconstruction. In *European conference on computer vision*, pages 231–248. Springer, 2022.
- [5] Hyungjin Chung, Byeongsu Sim, Dohoon Ryu, and Jong Chul Ye. Improving diffusion models for inverse problems using manifold constraints. *arXiv preprint arXiv:2206.00941*, 2022.
- [6] Enric Corona, Albert Pumarola, Guillem Alenyà, Francesc Moreno-Noguer, and Grégory Rogez. GanHand: Predicting human grasp affordances in multi-object scenes. In *CVPR*, pages 5030–5040, 2020.
- [7] Qi Dou, Daniel Coelho de Castro, Konstantinos Kamnitsas, and Ben Glocker. Domain generalization via model-agnostic learning of semantic features. *Advances in Neural Information Processing Systems*, 32, 2019.
- [8] Zicong Fan, Maria Parelli, Maria Eleni Kadoglou, Xu Chen, Muhammed Kocabas, Michael J Black, and Otmar Hilliges. Hold: Category-agnostic 3d reconstruction of interacting hands and objects from video. In *Proceedings of the IEEE/CVF Conference on Computer Vision and Pattern Recognition*, pages 494–504, 2024.
- [9] Zicong Fan, Omid Taheri, Dimitrios Tzionas, Muhammed Kocabas, Manuel Kaufmann, Michael J. Black, and Otmar Hilliges. ARCTIC: A dataset for dexterous bimanual hand-object manipulation. In *Proceedings IEEE Conference on Computer Vision and Pattern Recognition (CVPR)*, 2023.
- [10] Anindita Ghosh, Rishabh Dabral, Vladislav Golyanik, Christian Theobalt, and Philipp Slusallek. Imos: Intent-driven full-body motion synthesis for human-object interactions. In *Computer Graphics Forum*, volume 42, pages 1–12. Wiley Online Library, 2023.
- [11] Patrick Grady, Chengcheng Tang, Christopher D Twigg, Minh Vo, Samarth Brahmabhatt, and Charles C Kemp. Contactopt: Optimizing contact to improve grasps. In *Proceedings of the IEEE/CVF Conference on Computer Vision and Pattern Recognition*, pages 1471–1481, 2021.
- [12] Vladimir Guzov, Torsten Sattler, and Gerard Pons-Moll. Visually plausible human-object interaction capture from wearable sensors. *arXiv preprint arXiv:2205.02830*, 2022.
- [13] Shreyas Hampali, Mahdi Rad, Markus Oberweger, and Vincent Lepetit. Honnotate: A method for 3d annotation of hand and object poses. In *CVPR*, 2020.

- [14] Shreyas Hampali, Sayan Deb Sarkar, Mahdi Rad, and Vincent Lepetit. Keypoint transformer: Solving joint identification in challenging hands and object interactions for accurate 3d pose estimation. In *Proceedings of the IEEE/CVF Conference on Computer Vision and Pattern Recognition*, pages 11090–11100, 2022.
- [15] Yana Hasson, Bugra Tekin, Federica Bogo, Ivan Laptev, Marc Pollefeys, and Cordelia Schmid. Leveraging photometric consistency over time for sparsely supervised hand-object reconstruction. In *Proceedings of the IEEE/CVF conference on computer vision and pattern recognition*, pages 571–580, 2020.
- [16] Yana Hasson, Bugra Tekin, Federica Bogo, Ivan Laptev, Marc Pollefeys, and Cordelia Schmid. Leveraging photometric consistency over time for sparsely supervised hand-object reconstruction. In *CVPR*, pages 568–577, 2020.
- [17] Yana Hasson, Gül Varol, Cordelia Schmid, and Ivan Laptev. Towards unconstrained joint hand-object reconstruction from rgb videos. pages 659–668. IEEE, 2021.
- [18] Yana Hasson, Gul Varol, Dimitrios Tzionas, Igor Kalevatykh, Michael J Black, Ivan Laptev, and Cordelia Schmid. Learning joint reconstruction of hands and manipulated objects. In *Proceedings of the IEEE/CVF conference on computer vision and pattern recognition*, pages 11807–11816, 2019.
- [19] Yana Hasson, Gül Varol, Dimitrios Tzionas, Igor Kalevatykh, Michael J. Black, Ivan Laptev, and Cordelia Schmid. Learning joint reconstruction of hands and manipulated objects. In *CVPR*, pages 11807–11816, 2019.
- [20] Edward J Hu, Yelong Shen, Phillip Wallis, Zeyuan Allen-Zhu, Yanzhi Li, Shean Wang, Lu Wang, Weizhu Chen, et al. Lora: Low-rank adaptation of large language models. *ICLR*, 1(2):3, 2022.
- [21] Di Huang, Xiaopeng Ji, Xingyi He, Jiaming Sun, Tong He, Qing Shuai, Wanli Ouyang, and Xiaowei Zhou. Reconstructing hand-held objects from monocular video. In *SIGGRAPH Asia 2022 Conference Papers*, pages 1–9, 2022.
- [22] Janguang Jiang, Yang Shu, Jianmin Wang, and Mingsheng Long. Transferability in deep learning: A survey. *arXiv preprint arXiv:2201.05867*, 2022.
- [23] Korrawe Karunratanakul, Jinlong Yang, Yan Zhang, Michael J. Black, Krikamol Muandet, and Siyu Tang. Grasping Field: Learning implicit representations for human grasps. pages 333–344, 2020.
- [24] Taein Kwon, Bugra Tekin, Jan Stühmer, Federica Bogo, and Marc Pollefeys. H2o: Two hands manipulating objects for first person interaction recognition. In *Proceedings of the IEEE/CVF International Conference on Computer Vision*, pages 10138–10148, 2021.
- [25] Quanzhou Li, Jingbo Wang, Chen Change Loy, and Bo Dai. Task-oriented human-object interactions generation with implicit neural representations. *arXiv preprint arXiv:2303.13129*, 2023.
- [26] Shaowei Liu, Hanwen Jiang, Jiarui Xu, Sifei Liu, and Xiaolong Wang. Semi-supervised 3D hand-object poses estimation with interactions in time. In *CVPR*, pages 14687–14697, 2021.
- [27] Xueyi Liu and Li Yi. Geneoh diffusion: Towards generalizable hand-object interaction denoising via denoising diffusion. *arXiv preprint arXiv:2402.14810*, 2024.
- [28] Morteza Mardani, Jiaming Song, Jan Kautz, and Arash Vahdat. A variational perspective on solving inverse problems with diffusion models. *arXiv preprint arXiv:2305.04391*, 2023.
- [29] Chenlin Meng, Yutong He, Yang Song, Jiaming Song, Jiajun Wu, Jun-Yan Zhu, and Stefano Ermon. Sdedit: Guided image synthesis and editing with stochastic differential equations. In *International Conference on Learning Representations*, 2021.
- [30] Krikamol Muandet, David Balduzzi, and Bernhard Schölkopf. Domain generalization via invariant feature representation. In *International conference on machine learning*, pages 10–18. PMLR, 2013.

- [31] Johnny Núñez. *Comparison of Spatio-Temporal Hand Pose Denoising Models*. PhD thesis, Universitat DE Barcelona, 2022.
- [32] Aditya Prakash, Matthew Chang, Matthew Jin, and Saurabh Gupta. Learning hand-held object reconstruction from in-the-wild videos. *arXiv*, 2305.03036, 2023.
- [33] Charles Ruizhongtai Qi, Li Yi, Hao Su, and Leonidas J Guibas. Pointnet++: Deep hierarchical feature learning on point sets in a metric space. *Advances in neural information processing systems*, 30, 2017.
- [34] Wentian Qu, Zhaopeng Cui, Yinda Zhang, Chenyu Meng, Cuixia Ma, Xiaoming Deng, and Hongan Wang. Novel-view synthesis and pose estimation for hand-object interaction from sparse views. *arXiv preprint arXiv:2308.11198*, 2023.
- [35] Mattia Segu, Alessio Tonioni, and Federico Tombari. Batch normalization embeddings for deep domain generalization. *Pattern Recognition*, 135:109115, 2023.
- [36] Anthony Sicilia, Xingchen Zhao, and Seong Jae Hwang. Domain adversarial neural networks for domain generalization: When it works and how to improve. *Machine Learning*, pages 1–37, 2023.
- [37] Bowen Song, Soo Min Kwon, Zecheng Zhang, Xinyu Hu, Qing Qu, and Liyue Shen. Solving inverse problems with latent diffusion models via hard data consistency. *arXiv preprint arXiv:2307.08123*, 2023.
- [38] Anilkumar Swamy, Vincent Leroy, Philippe Weinzaepfel, Fabien Baradel, Salma Galaaoui, Romain Brégier, Matthieu Armando, Jean-Sebastien Franco, and Grégory Rogez. SHOWMe: Benchmarking object-agnostic hand-object 3d reconstruction. In *ICCV*, pages 1935–1944, 2023.
- [39] Omid Taheri, Nima Ghorbani, Michael J Black, and Dimitrios Tzionas. Grab: A dataset of whole-body human grasping of objects. In *Computer Vision–ECCV 2020: 16th European Conference, Glasgow, UK, August 23–28, 2020, Proceedings, Part IV 16*, pages 581–600. Springer, 2020.
- [40] Bugra Tekin, Federica Bogo, and Marc Pollefeys. H+O: Unified egocentric recognition of 3D hand-object poses and interactions. In *CVPR*, pages 4511–4520, 2019.
- [41] Purva Tendulkar, Dídac Surís, and Carl Vondrick. Flex: Full-body grasping without full-body grasps. In *Proceedings of the IEEE/CVF Conference on Computer Vision and Pattern Recognition*, pages 21179–21189, 2023.
- [42] Garvita Tiwari, Dimitrije Antić, Jan Eric Lenssen, Nikolaos Sarafianos, Tony Tung, and Gerard Pons-Moll. Pose-ndf: Modeling human pose manifolds with neural distance fields. In *Computer Vision–ECCV 2022: 17th European Conference, Tel Aviv, Israel, October 23–27, 2022, Proceedings, Part V*, pages 572–589. Springer, 2022.
- [43] Tze Ho Elden Tse, Kwang In Kim, Ales Leonardis, and Hyung Jin Chang. Collaborative learning for hand and object reconstruction with attention-guided graph convolution. In *CVPR*, pages 1664–1674, 2022.
- [44] Narek Tumanyan, Michal Geyer, Shai Bagon, and Tali Dekel. Plug-and-play diffusion features for text-driven image-to-image translation. In *Proceedings of the IEEE/CVF Conference on Computer Vision and Pattern Recognition*, pages 1921–1930, 2023.
- [45] Jindong Wang, Cuiling Lan, Chang Liu, Yidong Ouyang, Tao Qin, Wang Lu, Yiqiang Chen, Wenjun Zeng, and Philip Yu. Generalizing to unseen domains: A survey on domain generalization. *IEEE Transactions on Knowledge and Data Engineering*, 2022.
- [46] Pengfei Wang, Zhaoxiang Zhang, Zhen Lei, and Lei Zhang. Sharpness-aware gradient matching for domain generalization. In *Proceedings of the IEEE/CVF Conference on Computer Vision and Pattern Recognition*, pages 3769–3778, 2023.

- [47] Yan Wu, Jiahao Wang, Yan Zhang, Siwei Zhang, Otmar Hilliges, Fisher Yu, and Siyu Tang. Saga: Stochastic whole-body grasping with contact. In *Computer Vision–ECCV 2022: 17th European Conference, Tel Aviv, Israel, October 23–27, 2022, Proceedings, Part VI*, pages 257–274. Springer, 2022.
- [48] Xianghui Xie, Bharat Lal Bhatnagar, and Gerard Pons-Moll. Chore: Contact, human and object reconstruction from a single rgb image. In *Computer Vision–ECCV 2022: 17th European Conference, Tel Aviv, Israel, October 23–27, 2022, Proceedings, Part II*, pages 125–145. Springer, 2022.
- [49] Lixin Yang, Xinyu Zhan, Kailin Li, Wenqiang Xu, Jiefeng Li, and Cewu Lu. CPF: Learning a contact potential field to model the hand-object interaction. In *ICCV*, pages 11097–11106, 2021.
- [50] Lixin Yang, Xinyu Zhan, Kailin Li, Wenqiang Xu, Jiefeng Li, and Cewu Lu. CPF: Learning a contact potential field to model the hand-object interaction. In *ICCV*, 2021.
- [51] Yufei Ye, Abhinav Gupta, and Shubham Tulsiani. What’s in your hands? 3d reconstruction of generic objects in hands. In *CVPR*, 2022.
- [52] Yufei Ye, Abhinav Gupta, and Shubham Tulsiani. What’s in your hands? 3d reconstruction of generic objects in hands. In *Proceedings of the IEEE/CVF conference on computer vision and pattern recognition*, pages 3895–3905, 2022.
- [53] Yufei Ye, Poorvi Hebbar, Abhinav Gupta, and Shubham Tulsiani. Diffusion-guided reconstruction of everyday hand-object interaction clips. In *ICCV*, 2023.
- [54] Yufei Ye, Poorvi Hebbar, Abhinav Gupta, and Shubham Tulsiani. Diffusion-guided reconstruction of everyday hand-object interaction clips. In *Proceedings of the IEEE/CVF International Conference on Computer Vision*, pages 19717–19728, 2023.
- [55] Ruipeng Zhang, Qinwei Xu, Jiangchao Yao, Ya Zhang, Qi Tian, and Yanfeng Wang. Federated domain generalization with generalization adjustment. In *Proceedings of the IEEE/CVF Conference on Computer Vision and Pattern Recognition*, pages 3954–3963, 2023.
- [56] Yan Zhang and Siyu Tang. The wanderings of odysseus in 3d scenes. In *Proceedings of the IEEE/CVF Conference on Computer Vision and Pattern Recognition*, pages 20481–20491, 2022.
- [57] Kaiyang Zhou, Yongxin Yang, Yu Qiao, and Tao Xiang. Domain generalization with mixstyle. *arXiv preprint arXiv:2104.02008*, 2021.
- [58] Kanglei Zhou, Zhiyuan Cheng, Hubert PH Shum, Frederick WB Li, and Xiaohui Liang. Stgae: Spatial-temporal graph auto-encoder for hand motion denoising. In *2021 IEEE International Symposium on Mixed and Augmented Reality (ISMAR)*, pages 41–49. IEEE, 2021.
- [59] Keyang Zhou, Bharat Lal Bhatnagar, Jan Eric Lenssen, and Gerard Pons-Moll. Toch: Spatio-temporal object correspondence to hand for motion refinement. In *European Conference on Computer Vision (ECCV)*. Springer, October 2022.
- [60] Yuxiao Zhou, Marc Habermann, Weipeng Xu, Ikhsanul Habibie, Christian Theobalt, and Feng Xu. Monocular real-time hand shape and motion capture using multi-modal data. In *CVPR*, pages 5345–5354, 2020.